

Analysis of the electromeniscus phenomenon using a different interpretation of the Maxwell model applied to three-dimensional molecular orientations

Hiroshi Matsuura,¹ Hiromitsu Furukawa,² and Tsuyoshi Uda³

¹*Intelligent Systems Institute, National Institute of Advanced Industrial Science and Technology, Tsukuba 305-8564, Japan*

²*Photonics Research Institute, National Institute of Advanced Industrial Science and Technology, Tsukuba 305-8564, Japan*

³*Advanced Research Laboratory, Hitachi, Ltd., Kokubunji 185-8601, Japan*

(Received 25 October 2005; revised manuscript received 8 May 2006; published 19 June 2006)

An electrohydrodynamic phenomenon called the electromeniscus is analyzed. This phenomenon is closely related to the oscillation of a microscale liquid and is analyzed using an interpretation of the Maxwell model coupled with a variational principle. The analysis clearly shows that the electromeniscus phenomenon is generated as a result of mass transformation of the oscillating liquid in order to transform the electric energy at the electrode to kinetic energy of the liquid most efficiently through their resonance. Mass transformation is a characteristic phenomenon of a liquid, and control of this phenomenon demonstrates great potential for self-aligning nanoscale materials and production of functional polymers characterized by specific molecular orientations.

DOI: [10.1103/PhysRevE.73.066306](https://doi.org/10.1103/PhysRevE.73.066306)

PACS number(s): 47.54.-r, 47.85.L-, 05.65.+b, 45.70.Qj

I. INTRODUCTION

A remarkable step forward in nanotechnology occurred with the development of self-assembly techniques using a liquid [1,2]. Liquid is an inherently useful material for assembling many-body nanomaterials simultaneously [3] since liquid neutralizes excess electric charge on the materials and smoothly manipulates them with its surface tension [4,5]. The development of various driving forces for controlling the liquid dynamics also greatly contributed to the remarkable progress in self-assembling many-body nanomaterials [6–8].

The driving forces used in the self-assembly of nano- and micromaterials can be classified according to their form. An electromagnetic field has been most widely used for this purpose since this field is easier to analyze and control. Most research studies demonstrated a variety of two-dimensional assembly patterns with nano- and microparticles as a function of magnitude and frequency of the field [9,10]. Some studies showed that ordering of the particles was mainly affected by the interaction between the field and the particles, and the liquid simply behaved as a suspension [11]. Others, however, revealed that the electric-field-induced fluid flow generated by the concentration gradient of ions [12] or the interaction between charged granular gas and electrohydrodynamic convection flow [13,14] controlled the pattern formations of the particles. Other research proposed that the formation patterns of the particles in the field were governed by the competition between attractive forces among particles due to the electrohydrodynamic nature and repulsive force originating from electrical interactions among particles [15].

Other driving forces, such as vibration of the liquid [16,17], thermal gradient [18], evaporation of the liquid [3], and entropy of the many-particle systems [19], also produced various unique particle assembly patterns as a result of characteristic interactions between a liquid and particles. For example, vertical fluid vibration generated a streaming flow that served to produce long-range attractive interactions among non-Brownian particles, leading to self-assembly of a

variety of ordered and time-dependent dynamics of many-body particles [16].

These various forms of driving forces have successfully created unique assembly patterns with particles. However, most assemblies were restricted to two dimensions.

The focus of our current research is on three-dimensional self-assembly of nano- and microscale materials using microscale liquid dynamics induced by an intense electric field [20]. The liquid dynamics is called the electromeniscus phenomenon, and it has successfully performed carbon nanotube (CNT) erection and self-alignment of glass spheres three-dimensionally at any desired site on various substrates [21], which cannot be achieved by present self-assembly techniques. The phenomenon also demonstrated useful applications in developing further functional materials such as hydrogen-storing [22] and nitrogen-fixation [23] polymers. These results clearly show that the electromeniscus phenomenon has various potential applications and is particularly useful for self-aligning nano- and microscale materials three-dimensionally [20,21].

However, the mechanism of the electromeniscus phenomenon still remains unclear. The purpose of this paper is to clarify the mechanisms underlying this phenomenon using a generalized Maxwell model. First, the electromeniscus phenomenon is introduced. The phenomenon is then analyzed using the generalized Maxwell model coupled with a variational principle. This model clearly explains the mechanisms of the phenomenon in terms of mass transformation of the oscillating liquid. Finally, applications of the phenomenon, the CNT erection process, and formation of a thread polymer are demonstrated.

II. EXPERIMENT

The electromeniscus phenomenon was generated using the apparatus depicted in Fig. 1(a). The apparatus was placed in air, with temperature and humidity at 26 °C and 50%. An electrode pair was used and consisted of a sharpened tungsten electrode with a tip radius of 3 μm and a circular elec-

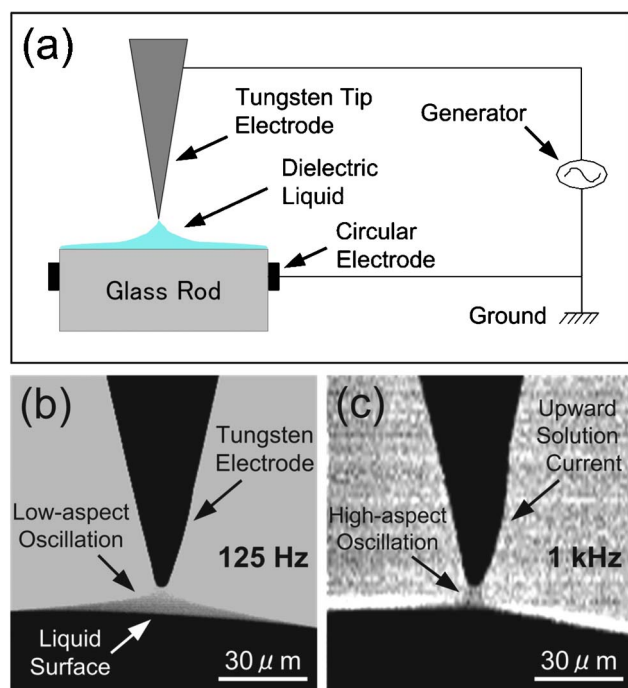


FIG. 1. (Color online) Observation of the electromeniscus phenomenon. (a) Apparatus for generating an electromeniscus. (b) Optical image of a low-aspect electromeniscus induced by a low-frequency electric field (125 Hz). (c) Optical image of a high-aspect electromeniscus induced by a high-frequency electric field (1 kHz). Solution 50-50 ethanol and distilled water. Purity of ethanol, 99.5% (Wako pure chemicals).

trode with an inner diameter of 1 mm. The circular electrode was attached to the side of a borosilicate glass rod with a diameter of 1 mm as shown in Fig. 1(a). The circular electrode was positioned 1 mm from the edge of the glass rod [Fig. 1(a)]. A solution consisting of 50-50 vol % of ethanol and distilled water was supplied on the side of the glass rod, forming a hemispherical liquid surface $50 \mu\text{m}$ thick. A generator was connected between the electrodes, and a sinusoidal electric potential of 0.5 kV was applied.

When a sinusoidal electric potential of 125 Hz was applied, the liquid surface oscillated as a flattened triangular pyramid [Fig. 1(b), black arrows]. However, the oscillating area transformed into a high-aspect meniscus and flew up as an upward current along the tungsten electrode when the frequency was increased to 1 kHz [Fig. 1(c), black arrows]. We call this transition of liquid dynamics the electromeniscus phenomenon [21]. The electromeniscus continued to oscillate at the same frequency as the applied electric potential during the geometry transition.

III. ANALYSIS OF THE PHENOMENON

A. Formation of the high-aspect electromeniscus

Analysis of this electromeniscus phenomenon involves some inherent difficulties originating from the characteristic properties of a microscale liquid. Specifically, a liquid at this scale possesses not only viscosity but also elasticity due to its intense surface tension. The transition of the liquid geom-

etry in Fig. 1 as a function of the electric frequency also makes the analysis more difficult. Therefore, we developed a generalized Maxwell model both to avoid those difficulties and to clarify the mechanisms of this electromeniscus phenomenon.

The generalized Maxwell model consists of a linear chain of spring, damper, and weight of variable mass, whereas the “original” Maxwell model [24] has a fixed mass. A spring and damper are arranged to represent the surface tension force and viscosity of the microscale liquid in Fig. 1. The variable mass of the weight is a characteristic element in this model and is employed for describing a mass transformation of the liquid in Fig. 1 as a function of the electric frequency. The variable mass is expected to represent the transition of the liquid geometry in Fig. 1 in terms of mass transformation of the liquid.

The equation of motion for the generalized Maxwell model is described as [21]

$$m(\omega) \frac{d^2 z}{dt^2} = -kz - \gamma \frac{dz}{dt} + f_0 \cos \omega t. \quad (1)$$

Here $m(\omega)$ represents the variable mass of the weight as a function of the frequency of the external force instead of the fixed mass m as used in the original Maxwell model. z , t , and k are the displacement of the weight, the time, and a spring constant. γ , f_0 , and ω are the attenuation coefficient of the damper, the amplitude of the external force, and the angular frequency of the weight.

The left side of the equation represents the force acting on the weight. The first, second, and third terms on the right side of the equation are the restoring force of the spring, the damping force, and the external force on the weight. Equation (1) demonstrates that, during the oscillation of the weight, the external energy is transformed into kinetic energy in the weight and potential energy in the spring, with these energies consumed as heat loss due to the viscosity of the damper. During these energy transformations, a weight with variable mass will transform its mass as a function of the frequency of the external force in order to achieve the most stable state.

This generalized Maxwell model with a variable-mass weight would be useful in describing the transition of the liquid geometry in Fig. 1 in terms of mass transformation, with the terms in Eq. (1) corresponding to the kinetic energy of the liquid (left side of the equation), the surface energy of the liquid, the sum of the internal energy and heat loss of the liquid, and the electric force on the liquid surface in Fig. 1. With this correspondence, Eq. (1) can be interpreted as indicating that during the oscillation of the liquid the electric energy between the electrodes in Fig. 1 is transformed into kinetic energy of the liquid and surface energy on the liquid surface, with these energies consumed as heat loss due to the viscosity of the liquid. During these energy transformations, the oscillating liquid will transform the mass as a function of the electric frequency in order to most efficiently consume the electric energy as kinetic energy in the liquid, thus achieving the most stable state.

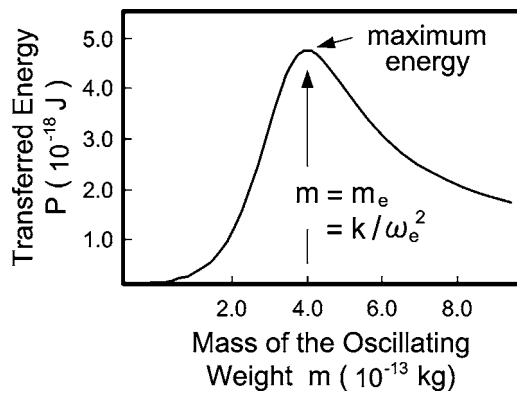


FIG. 2. Transferred energy from an external force to the weight as a function of the mass of the oscillating weight. The simulation is derived from Eq. (2). The maximum energy is achieved when the mass of the oscillating weight, m , takes on the eigenvalue of the weight, k/ω_e^2 , and the oscillation of the weight resonates with the external force.

In this generalized Maxwell model, we ignore the nonlinearity of the liquid oscillation, assuming that the surface tension force and the viscosity of the liquid can be described by a linear function of displacement kz and the velocity of the weight $\gamma dz/dt$. Because of these approximations, the model may not be suitable for quantitatively describing the actual liquid dynamics in Fig. 1. However, this model, with its variable-mass weight, will qualitatively describe the core mechanisms for the geometry transition of the liquid in terms of mass transformation.

To explain the transition of the liquid geometry in Fig. 1 in terms of mass transformation of the weight, we analyze the amount of energy transferred from an external force to the weight based on the generalized Maxwell model.

The average amount of transferred energy P in a period of oscillation was derived from Eq. (1) as [21]

$$P = \frac{\gamma\omega^2}{2\left(\frac{k}{m} - \omega^2\right)^2 + \frac{2}{m^2}\gamma\omega^2} f_0^2. \quad (2)$$

Here, γ , k , and f_0 are assumed to be constant in this model while m is considered a function of the frequency of the external force, ω . k/m in the denominator then becomes a function of the frequency of the external force, ω , corresponding to the square of the eigen frequency of the weight with variable mass, ω_e^2 , i.e., $k/m = \omega_e^2$.

Figure 2 represents the transferred energy P as a function of the mass of the oscillating weight $m(\omega)$. This figure was simulated from Eq. (2) with the variables γ , k , ω , and f_0 set to 10^{-14} , 10^{-3} , $2\pi \times 10^3$, and 10^2 . The maximum energy in Fig. 2 is achieved when the denominator of Eq. (2) becomes a minimum with the mass of the weight, $m(\omega)$, taking on the eigenvalue of the weight, k/ω_e^2 , and achieving a resonance with the external force.

We note that there is no restriction in Eq. (2) for specifying the mass of the oscillating weight: The mass of the weight is able to take any value along the x axis in Fig. 2. This contradicts the experimental results in Fig. 1 where the

mass of the oscillating liquid took on a specific value as a function of the electric frequency. Therefore, a fundamental principle is necessary for specifying the mass of the oscillating weight as a function of the frequency of the external force.

Here, we apply a variational principle to Eq. (2) to determine the mass of the oscillating weight, m , in Fig. 2 as a function of the frequency of the external force, ω . The principle is a fundamental law of nature for deciding how matter will behave, stating that the motion of matter is determined such that a critical variable of the system takes either a minimum or maximum amount [25].

Although the variational principle is generally applied to the equilibrium state, it is also possible to apply it to a non-equilibrium state like that of the liquid oscillation in Fig. 1. When applying the principle to the oscillation in Fig. 1, the maximum energy in Fig. 2 (black arrow) becomes time dependent and thus determining the steady mass m as a function of the frequency of the external force, ω , would be difficult. However, the liquid oscillates at the same frequency as the applied electric field (Fig. 1) and could thus be considered to be in a nonequilibrium steady state. In this state, the variational principle combined with the forced oscillation theory is able to determine the steady mass of the oscillating weight in Fig. 2 as a function of the frequency of the external force.

In a nonequilibrium steady state, the principle is interpreted as stating that the mass of the oscillating weight in Fig. 2 will be determined such that the transferred energy P becomes maximum when the oscillation of the weight most efficiently consumes the external energy as kinetic energy in the weight. According to the forced oscillation theory [24], the most efficient process for consuming external energy (electric energy, in the case of Fig. 1) is one where the external energy is in resonance with another oscillator or weight (or liquid, in Fig. 1). Therefore, the oscillating liquid in Fig. 1 would need to be in a resonant state with an electric field to achieve the most stable state possible.

In fact, the electromeniscus in Fig. 1 is considered to be in the resonant state or close to resonance with the applied electric field. The electromeniscuses in Figs. 1(b) and 1(c) oscillated with masses of 1.4×10^{-11} and 5.3×10^{-13} kg. Therefore, the eigenfrequencies of these meniscuses are estimated as 0.42 and 2.45 kHz, which correspond to applied electric fields of 0.125 and 1 kHz. Here, the eigenfrequencies were calculated from the square root of k/m [24], where the spring constant k was approximated as a surface tension of 50-50 water-ethanol at $\sim 10^{-3}$ N/m. This agreement certainly shows that the electromeniscuses in Fig. 1 would be in a resonant state or in a state close to resonance with the applied electric fields.

Based on these analyses, the mass of the oscillating weight, m , as a function of the frequency of the external force, ω , is determined from the variational principle such that the transferred energy P in Fig. 2 becomes maximum. The determination is achieved by taking the derivative of Eq. (2) with respect to the frequency of the external force and setting that derivative to zero ($\partial P/\partial \omega = 0$).

The calculation was performed computationally and the relationship between the mass of the oscillating weight,

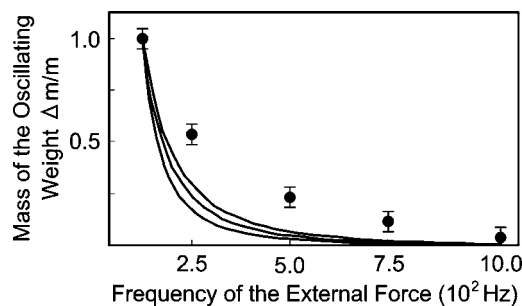


FIG. 3. Transition of the mass of the oscillating weight as a function of the frequency of the external force. Solid lines represent the simulations of the mass transformations of the weight when the spring constant k is 1×10^{-4} , 5×10^{-4} and 10×10^{-4} N/m, reading from the left. Black spots represent the mass of the oscillating liquid in Fig. 1 when electric frequencies are 125, 250, 500, 750, and 1000 Hz. The masses of both simulations and experiments are reduced in inverse proportion as the frequency of the external force is increased.

$m(\omega)$, and frequency of the external force, ω , in shown in Fig. 3. The X and Y axes represent the frequency of the external force and the mass of the oscillating weight. The mass of the weight in this figure was converted to a ratio in order that the original mass is represented as a mass of 1.

The solid lines in Fig. 3 indicate the mass transformations of the oscillating weight as a function of the frequency of the external force with values for the spring constant k of 1×10^{-4} , 5×10^{-4} , and 1×10^{-3} N/m, reading from the left. These spring constants were approximated based on the surface tension of 50-50 water-ethanol at 10^{-3} N/m. The attenuation coefficient γ and the amplitude of the external force f_0 were assumed to be 10^{-14} and 10^2 in this simulation.

The black spots in Fig. 3 represent the masses of the electromeniscus in Fig. 1. The masses are 1.4×10^{-11} kg at 125 Hz, 7.5×10^{-12} kg at 250 Hz, 3.3×10^{-12} kg at 500 Hz, 1.6×10^{-12} kg at 750 Hz, and 5.3×10^{-13} kg at 1000 Hz. These masses were converted from their volumes, which were calculated from the magnified optical images in Fig. 1. For example, the volume was approximated as a triangular pyramid for a low-aspect electromeniscus, but as a cylinder for a high-aspect electromeniscus. The masses of the electromeniscuses were also converted to a ratio in order that the original mass is represented as a mass of 1. The vertical lines on each spot represent the range of errors.

A comparison between the simulations and the experimental results in Fig. 3 reveals some quantitative discrepancies as estimated before. For example, the mass reduction ratio around 250 Hz in the model is much greater than that of the actual liquid. Moreover, the simulated mass erroneously decreases to zero at around 750 Hz.

These discrepancies arise from the neglect of nonlinearity in the liquid oscillation in our model (i.e., the spring constant k and the attenuation coefficient of the damper, γ , were assumed to be constant during the oscillation) [21]. These amounts could be complicated functions of the displacement of the weight, $k(z)$, and the velocity of the weight, $\gamma(dz/dt)$, because of the geometry transition of the liquid as a function of space and time during the oscillation in Fig. 1. The model

parameters such as k , γ , and f_0 might also affect the disagreement. As indicated above, the model will undergo several improvements for the quantitative explanation of the experimental results in Fig. 3.

However, the simulation in Fig. 3 qualitatively reproduces a similar tendency in the experimental results without requiring any dubious assumptions: the mass of the oscillating weight is reduced in inverse proportion to the frequency of the external force. This qualitative agreement, being obtained without any dubious approximations, supports the idea that our approach, based on the generalized Maxwell model coupled with a variational principle, is appropriate for describing the core mechanisms underlying the geometry transition of the liquid in Fig. 1.

In fact, the result in Fig. 3 clearly explains the transition of the liquid geometry in Fig. 1 in terms of mass transformation of the weight: the mass transformation of the weight in Fig. 3 as a function of the frequency of the external force corresponds to the mass transformation of the liquid in Fig. 1, which accompanies the geometry transition of the liquid, as a function of the frequency of the electric field.

Based on these analyses, the overall mechanism for the transition of the liquid geometry, which is the electromeniscus phenomenon in Fig. 1, can be described as follows. The phenomenon is generated as a result of mass transformation of an oscillating liquid in order that the electric energy from the tungsten tip transforming to kinetic energy of the liquid achieves a maximum through resonance between the electric field and the liquid, causing it to take the most stable state.

B. Formation of the upward solution current

The mechanism of another important dynamic of the electromeniscus phenomenon, i.e., the formation of an upward solution current along the tungsten electrode [Fig. 1(c), black arrow], was also analyzed.

The upward current was generated when the applied electric frequency was increased as indicated in Figs. 1(b) and 1(c). Therefore, the kinetic energy of the oscillating liquid and the temperature gradient around the tungsten tip are closely related to the formation of the current. In particular, the kinetic energy of the oscillating liquid is a driving force both to carry the solution from the glass rod and to release the solution onto the tungsten tip. At the same time, according to the Marangoni effect [5,26], the temperature gradient around the tungsten tip has a strong potential to make the solution released onto the tip migrate upward along the tip.

We will first evaluate the transport and release of the solution. To transport and release the solution from the liquid surface to the tungsten tip, the kinetic energy of the electromeniscus per unit area must exceed the surface tension of the meniscus. A comparison of the magnitudes of the kinetic energy per unit area and the surface tension demonstrated the following reasonable results. The electromeniscus in Fig. 1(c), whose mass was 5.3×10^{-13} kg, oscillated by $10 \mu\text{m}$ at 1 kHz. Thus, the average kinetic energy of this meniscus was calculated as 2.65×10^{-15} J. Since the average radius of the meniscus was $2.5 \mu\text{m}$, the kinetic energy of the meniscus per unit area was estimated as 1.35×10^{-2} J/m². This estimate

certainly demonstrates that the kinetic energy of the electromeniscus per unit area exceeded 10^{-3} N/m, which is the surface tension of the solution in Fig. 1 (50-50 vol % of ethanol and distilled water). The kinetic energy in the electromeniscus exceeded the surface tension and must have carried the solution onto the tungsten electrode in Fig. 1(c).

Meanwhile, the electromeniscus in Fig. 1(b) oscillated the same distance ($10\ \mu\text{m}$) at 125 Hz. Therefore, the average kinetic energy of this electromeniscus per unit area was estimated as 2.1×10^{-4} J/m² at maximum, considering the same cross section of the electromeniscus as in Fig. 1(c). In this case, the kinetic energy of the meniscus per unit area (2.1×10^{-4} J/m²) was less than the surface tension of the solution (10^{-3} N/m). The surface tension of the solution, being greater than the kinetic energy of the electromeniscus, must have inhibited the carrying of the solution to the tungsten tip as shown in Fig. 1(b).

Quantitative evaluation of the Marangoni effect caused by the temperature gradient around the tungsten tip is difficult at present because making reliable temperature measurements at the tungsten tip is not easy. However, based on previous research [5,26], Marangoni effects caused by gradients of temperature, electric field, or concentration become substantial driving forces, especially for microscale liquids. Therefore, the Marangoni effect would contribute to the migration of the microscale solution carried upward along the tungsten electrode toward the tungsten tip as seen in Fig. 1. In this paper, we qualitatively estimate the mechanism of this migration of the transported solution as follows.

According to electromagnetic theory [27,28], a certain percentage of energy in the form of an electric current is consumed as heat loss in an Ohmic material. Since heat loss is a linear function of the current [27,28], the percentage of heat loss at a smaller dimension is greater than at a larger dimension. Therefore, a temperature gradient from the tip of the tungsten electrode toward the base will be generated as long as an electric frequency is applied to the electrode.

When the electric frequency is increased by a factor of 8, for example from 125 Hz to 1 kHz as in Fig. 1, the current also increases in the same ratio. Since tungsten is an Ohmic material, the heat loss due to its resistivity increases by eight times [27,28]. If the temperature of the base of the tungsten electrode is held constant, only the temperature around the tip will be enhanced. This scenario is realistic when the base of the tungsten electrode is large enough that the heat loss at the base can be ignored. In this case, the temperature gradient from the tip to the base of the tungsten electrode in Fig. 1 will be enhanced eight times when the electric frequency is increased by a factor of 8.

According to the Marangoni effect, the solution migrates from the hotter area toward the cooler area [5,26]. Thus, the migration of the upward solution current from the tip of the tungsten electrode toward the base as shown in Fig. 1(c) can be qualitatively explained by the Marangoni effect.

These analyses support the idea that kinetic energy transports the solution onto the tungsten electrode and that the Marangoni effect causes this transported solution to migrate upward along the electrode. A series of these processes would form an upward solution current along the tungsten electrode as seen in Fig. 1(c).

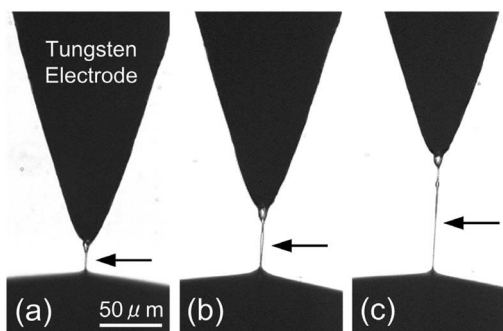


FIG. 4. Optical image of thread polymer composed from alcohol. (a) Alcohol thread polymer right after composition using the electromeniscus phenomenon with electron emission. (b) Polymer stretched by $30\ \mu\text{m}$ from length in image (a) without electric field. (c) Polymer stretched by $50\ \mu\text{m}$ from length in image (b) without electric field. The alcohol thread polymer was composed only when electron emission was applied to the electromeniscus with an intense electric potential (3.5 kV).

IV. APPLICATION OF THE PHENOMENON

This formation of a high-aspect electromeniscus and upward solution current has various potential applications ranging from physics to chemistry. In the field of physics, measuring the properties of a carbon nanotube is still an important issue. However, there are no appropriate methods to manipulate a CNT at present due to its intense surface tension. The application of the electromeniscus phenomenon made it possible to erect a CNT on a substrate [21, supporting information]. Once a CNT is erected, it becomes possible to adjust its positions and easier to measure its electrical and optical properties.

The current research also revealed that control of the electromeniscus makes it possible to synthesize a thread polymer from 1-butanol (a kind of alcohol). Figure 4 represents the stretching of the polymer after the electromeniscus phenomenon. The polymer thread exhibited a stretching ratio of more than 1000%.

Figure 4(a) presents a $25\ \mu\text{m}$ thread polymer (black arrow) synthesized between a tungsten electrode and a substrate. The polymer was composed when a 3.5 kV, 16 kHz high-frequency electric potential was applied for 8 s during the formation of the electromeniscus in Fig. 1(c), using 1-butanol instead of 50-50 vol % of ethanol and distilled water. Since the polymer was formed only when an electric current ($26\ \mu\text{A}$) was generated, the polymer was composed as a result of an interaction between alcohol molecules and electron emission from the tungsten electrode.

In our previous work, we observed alcohol polymerization using electron emission from an atomic force microscope (AFM) tip with relatively low potential (1.2 kV), [21, see supporting information]. However, these polymers were either a liquid or a thin film [22,23]. The thread polymer shown in Fig. 4 was not obtained as long as the AFM tip with 1.2 kV of electric potential was used.

These results clearly demonstrate that the electron emission itself is not sufficient for composing the alcohol-based thread polymer in Fig. 4. Decomposition of the molecules

with electron emission and subsequent rearrangement of the molecules along the intense electric field is also necessary to compose such a thread polymer. The formation of the electromeniscus in an intense electric field must have created these ideal conditions. An intense electric field at the electrode generated electron emission toward the electromeniscus, decomposed the molecules composing the meniscus, and rearranged the dissociated molecules parallel to the electric field. A series of these processes would make it possible to compose the thread polymer in Fig. 4.

At this point, the molecular structure of this thread polymer is not clear. However, the formation process of the polymer parallel to such an intense electric field and the unusual stretching ratio in Fig. 4 strongly suggest that the polymer must have a certain molecular orientation along the electric field during the process.

The application of CNTs to the formation process of this thread polymer will make it possible to fabricate more useful composite materials with unique electrical and optical properties [29,30].

V. CONCLUSION

We have analyzed the mechanism underlying the geometry transition of an oscillating liquid as a function of the electric frequency. This electromeniscus phenomenon was analyzed using a generalized Maxwell model involving a weight of variable mass to represent the geometry transition of the liquid in terms of mass transformation. In this model, the amount of mass transformation was determined from the variational principle taking the most stable state where the transferred energy from the external force to the weight achieves a maximum. These approaches, based on a generalized Maxwell model coupled with a variational principle, qualitatively explained the experimental results without requiring any dubious assumptions. Therefore, we assume the core mechanisms of the electromeniscus phenomenon to be as follows. The phenomenon, which accompanies a geometry transition of an oscillating liquid, is generated as a result of mass transformation of the liquid in order to achieve the most stable state by transforming the electric energy at the electrode to kinetic energy of the liquid most efficiently through their resonance.

From a scientific point of view, development of the generalized Maxwell model involving a variable-mass weight was an important step since the model revealed an essential liquid dynamic, i.e., a mass transformation of an oscillating liquid as a function of electric frequency, which the original Maxwell model with its fixed mass could never explain. The application of the variational principle was also useful for clarifying the relationship among the most stable state of the oscillating liquid, the mass transformation of the liquid, and resonance between the electric field and the liquid without analyzing the detailed formation process of the electromeniscus.

The formation mechanisms of the upward solution current along the tungsten electrode were analyzed based on an evaluation of the kinetic energy of the oscillating liquid and the Marangoni effect. A comparison between the surface tension and the kinetic energy of the solution per unit area demonstrated that the solution would be transported and released onto the tungsten electrode when the kinetic energy of the solution per unit area exceeded the surface tension of the solution. In addition, qualitative analysis based on the Marangoni effect indicated that the temperature gradient from the tip of the tungsten electrode to the base would cause the transported solution to migrate from the tip to the base of the electrode. The combined driving force of the kinetic energy and the Marangoni effect would form an upward solution current along the tungsten electrode.

A CNT erection process and formation of alcohol-based thread polymer demonstrated possible applications of the electromeniscus phenomenon. These results clearly show that the phenomenon has great potential for providing specific three-dimensional orientations to molecules and nanomaterials.

The molecular orientation and the optical and electrical properties of the thread polymer composed during the electromeniscus phenomenon will be reported in the future.

ACKNOWLEDGMENTS

We thank Dr. T. Tanikawa and Dr. M. Ogawa for helpful discussions. This work was supported by the Intelligent Systems Institute, National Institute of Advanced Industrial Science and Technology.

-
- [1] R. C. Hayward, D. A. Saville, and I. A. Aksay, *Nature (London)* **404**, 56 (2000).
 - [2] N. Bowden, A. Terfort, J. Carbeck, and G. M. Whitesides, *Science* **276**, 233 (1997).
 - [3] L. V. Govor, G. Reiter, J. Parisi, and G. H. Bauer, *Phys. Rev. E* **69**, 061609 (2004).
 - [4] D. E. Kataoka and S. M. Troian, *Nature (London)* **402**, 794 (1999).
 - [5] N. Garnier, R. O. Grigoriev, and M. F. Schatz, *Phys. Rev. Lett.* **91**, 054501 (2003).
 - [6] M. G. Pollack and R. B. Fair, *Appl. Phys. Lett.* **77**, 1725 (2000).
 - [7] A. A. Darhuber, J. P. Valentino, J. M. Davis, and S. M. Troian, *Appl. Phys. Lett.* **82**, 657 (2003).
 - [8] S. Duhr and D. Braun, *Appl. Phys. Lett.* **86**, 131921 (2005).
 - [9] W. D. Ristenpart, I. A. Aksay, and D. A. Saville, *Phys. Rev. E* **69**, 021405 (2004).
 - [10] M. V. Sapozhnikov, I. S. Aranson, W. K. Kwok, and Y. V. Tolmachev, *Phys. Rev. Lett.* **93**, 084502 (2004).
 - [11] M. F. Islam, K. H. Lin, D. Lacoste, T. C. Lubensky, and A. G. Yodh, *Phys. Rev. E* **67**, 021402 (2003).
 - [12] S. R. Yeh, M. Seul, and B. I. Shraiman, *Nature (London)* **386**, 57 (1997).
 - [13] M. V. Sapozhnikov, Y. V. Tolmachev, I. S. Aranson, and W. K.

- Kwok, Phys. Rev. Lett. **90**, 114301 (2003).
- [14] I. S. Aranson and M. V. Sapozhnikov, Phys. Rev. Lett. **92**, 234301 (2004).
- [15] F. Nadal, F. Argoul, P. Hanusse, and B. Pouligny, Phys. Rev. E **65**, 061409 (2002).
- [16] G. A. Voth, B. Bigger, M. R. Buckley, W. Losert, M. P. Brenner, H. A. Stone, and J. P. Gollub, Phys. Rev. Lett. **88**, 234301 (2002).
- [17] C. C. Thomas and J. P. Gollub, Phys. Rev. E **70**, 061305 (2004).
- [18] S. Duhr and D. Braun, Appl. Phys. Lett. **86**, 131921 (2005).
- [19] B. Mayer, G. Hohler, and S. Rasmussen, Phys. Rev. E **55**, 4489 (1997).
- [20] H. Matsuura, M. Miyazaki, M. Komatsu, and M. Ogawa, Appl. Phys. Lett. **87**, 134106 (2005).
- [21] See EPAPS Document No. E-PLLEE8-73-140606 (<http://ftp.aip.org/cgi-bin/epaps?ID=E-PLLEE8-73-140606>) for supporting information (applications of the electromeniscus phenomenon and the derivation of fundamental equations in the manuscript). For more information on EPAPS, see <http://www.aip.org/pubserve/epaps.html>.
- [22] H. Matsuura, T. Tanikawa, H. Takaba, and Y. Fujiwara, J. Phys. Chem. A **108**, 3235 (2004).
- [23] H. Matsuura, T. Tanikawa, H. Takaba, and Y. Fujiwara, J. Phys. Chem. B **108**, 17748 (2004).
- [24] I. Bloch, *The Physics of Oscillations and Waves: With Applications in Mechanics and Electricity* (Solomon, 1994).
- [25] L. N. Hand and J. D. Finch, *Analytical Mechanics* (Cambridge University Press, Cambridge, U.K., 1998).
- [26] M. F. Schatz and G. P. Neitzel, Annu. Rev. Fluid Mech. **33**, 93 (2001).
- [27] I. Imai, J. Phys. Soc. Jpn. **60**, 4100 (1991).
- [28] I. Imai, *A New Approach to Electromagnetic Theory* (Saiensu-sya, Tokyo, 1990).
- [29] X. Zhang, T. Liu, T. V. Sreekumar, S. Kumar, V. C. Moore, R. H. Hauge, and R. E. Stanley, Nano Lett. **3**, 1285 (2003).
- [30] Y. Kim, N. Minami, and S. Kazai, Appl. Phys. Lett. **86**, 073103 (2005).